arXiv:0909.1114v1 [nucl-th] 6 Sep 2009

Quark-hadron phase transition in a neutron star under strong magnetic fields

A. Rabhi,[1, 2, *] H. Pais,[1, †] P. K. Panda,[3, 1, ‡] and C. Providência[1, §]
[1] *Centro de Física Computacional, Department of Physics,*
University of Coimbra, 3004-516 Coimbra, Portugal
[2] *Laboratoire de Physique de la Matière Condensée,*
Faculté des Sciences de Tunis, Campus Universitaire, Le Belvédère-1060, Tunisia
[3] *Indian Association for the Cultivation of Sciences, Jadavpur, Kolkata-700 032, India*

(Dated: September 6, 2009)

We study the effect of a strong magnetic field on the properties of neutron stars with a quark-hadron phase transition. It is shown that the magnetic field prevents the appearance of a quark phase, enhances the leptonic fraction, decreases the baryonic density extension of the mixed phase and stiffens the total equation of state, including both the stellar matter and the magnetic field contributions. Two parametrisations of a density dependent static magnetic field, increasing, respectively, fast and slowly with the density and reaching $2-4\times10^{18}$G in the center of the star, are considered. The compact stars with strong magnetic fields have maximum mass configurations with larger masses and radius and smaller quark fractions. The parametrisation of the magnetic field with density has a strong influence on the star properties.

PACS numbers: 26.60.+c, 12.39.Ba, 21.65.+f, 97.60.Jd

I. INTRODUCTION

Neutron stars with very strong magnetic fields of the order of $10^{14}-10^{15}$ G are known as magnetars and they are believed to be the sources of the intense gamma and X rays [1–3]. If the magnetic field at the center of the star has the same magnitude as the one measured at the surface of a magnetar, then the influence of the magnetic field on the star's mass and radius is negligible. However, according to the scalar virial theorem the maximum interior field strength could be as large as 10^{18} G for a compact star [4]. For a field of this magnitude or larger considerable effects will be induced on EOS.

It has been shown by several authors that the magnetic fields larger than $B = 5\times10^{18}$ G will affect the EOS of compact stars [5, 6]. In particular field-theoretical descriptions based on the non-linear Walecka model (NLWM) [7] were used. The generalization of these works to density-dependent hadronic models [8] or the inclusion of the scalar-isovector δ mesons [9] have also been applied to the description of hadronic stars with intense magnetic fields. Quark stars with strong magnetic fields have been described within the MIT bag model [5, 10, 11] and the SU(2) version of the Nambu–Jona–Lasinio model (NJL) [12], an effective model which includes the chiral symmetry, a symmetry of QCD.

Compact stars are complex systems which may contain in their core a pure quark phase or a non-homogenous mixed quark-hadron phase [13]. We would like to investigate whether the presence of a magnetic field could affect the presence of a quark core. The influence of strong magnetic fields on quark-hadron phase transition was first discussed in Ref. [14], using a Dirac-Hartree-Fock approach within a mean-field approximation to describe both the hadronic and quark phases. For the hadronic matter they took a system of protons, neutrons and electrons and for the quark phase the MIT bag model with one-gluon exchange. A very hard quark EOS was used so that the hybrid star did not have a quark core. They have concluded that compact stars have a smaller maximum mass in the presence of strong magnetic fields, a result that does not agree with other works where hadronic stars [15] or quark stars [12] in the presence of strong magnetic fields, have been studied.

In the present work we will study the effect of a strong magnetic field on the deconfinement phase transition inside a compact star. We will consider two EOS for the quark phase, a softer and a harder one, chosen in such a way that the star will have at least a small quark core if no magnetic field exists. For the hadronic phase we consider a standard hadronic EOS, the GM1 parametrisation of the non-linear Walecka model proposed in [16], and include

---

[*] Electronic address: `rabhi@teor.fis.uc.pt`
[†] Electronic address: `pais.lena@gmail.com`
[‡] Electronic address: `prafulla.k.panda@gmail.com`
[§] Electronic address: `cp@teor.fis.uc.pt`

the baryonic octet. The largest magnetic field measured at the surface of a star is $\sim 10^{15}$ G but nothing is known about the magnitude of magnetic fields in the interior of a star. We will consider a magnetic field whose magnitude increases from a value of $\sim 10^{15}$ at the surface to a maximum value of $\sim 4 \times 10^{18}$ G at the center. In particular, we want to analyse how the parametrisation of the field affects the star properties, such as the radius and mass.

This work is organized as follows: we make a brief review of the formalism used for the hadronic, mixed and quark phases. Next we discuss the parametrisation used for the magnetic field and present and discuss the results obtained for the equation of state of stellar matter and the mass/radius properties of the corresponding compact star families, for several values of the maximum magnetic field. At the end we will draw some conclusions.

II. HADRON MATTER EQUATIONS OF STATE

For the description of the EOS of neutron star matter, we employ a field-theoretical approach in which the baryons interact via the exchange of $\sigma - \omega - \rho$ mesons in the presence of a static magnetic field B along the z-axis. The Lagrangian density of the NLW model (GM1) can be written as

$$\mathcal{L} = \sum_b \mathcal{L}_b + \mathcal{L}_m + \sum_l \mathcal{L}_l. \tag{1}$$

The baryons, leptons (l=e, μ), and mesons (σ, ω and ρ) Lagrangians are given by

$$\begin{aligned}
\mathcal{L}_b &= \bar{\Psi}_b \left(i\gamma_\mu \partial^\mu - q_b \gamma_\mu A^\mu - m_b + g_{\sigma b}\sigma - g_{\omega b}\gamma_\mu \omega^\mu - g_{\rho b}\tau_{3_b}\gamma_\mu \rho^\mu - \frac{1}{2}\mu_N \kappa_b \sigma_{\mu\nu} F^{\mu\nu} \right) \Psi_b \\
\mathcal{L}_l &= \bar{\psi}_l \left(i\gamma_\mu \partial^\mu - q_l \gamma_\mu A^\mu - m_l \right) \psi_l \\
\mathcal{L}_m &= \frac{1}{2}\partial_\mu \sigma \partial^\mu \sigma - \frac{1}{2} m_\sigma^2 \sigma^2 - U(\sigma) + \frac{1}{2} m_\omega^2 \omega_\mu \omega^\mu - \frac{1}{4}\Omega^{\mu\nu}\Omega_{\mu\nu} \\
&- \frac{1}{4} F^{\mu\nu} F_{\mu\nu} + \frac{1}{2} m_\rho^2 \rho_\mu \rho^\mu - \frac{1}{4} P^{\mu\nu} P_{\mu\nu}
\end{aligned} \tag{2}$$

where Ψ_b and ψ_l are the baryon and lepton Dirac fields, respectively. The index b runs over the eight lightest baryons n, p, Λ, Σ^-, Σ^0, Σ^+, Ξ^- and Ξ^0. (Neglecting the baryonic decuplet including the Ω^- and the Δ quartet, which appear only at very high densities, does not affect our conclusions). The baryon mass and isospin projection are denoted by m_b and τ_{3_b}, respectively. The mesonic and electromagnetic field tensors are given by their usual expressions: $\Omega_{\mu\nu} = \partial_\mu \omega_\nu - \partial_\nu \omega_\mu$, $P_{\mu\nu} = \partial_\mu \rho_\nu - \partial_\nu \rho_\mu$, and $F_{\mu\nu} = \partial_\mu A_\nu - \partial_\nu A_\mu$. The baryon anomalous magnetic moments (AMM) are introduced via the coupling of the baryons to the electromagnetic field tensor with $\sigma_{\mu\nu} = \frac{i}{2}\left[\gamma_\mu, \gamma_\nu\right]$ and strength κ_b. The electromagnetic field is assumed to be externally generated (and thus has no associated field equation), and only frozen-field configurations will be considered. The interaction couplings are denoted by g, the electromagnetic couplings by q and the baryons, mesons and leptons masses by m. The scalar self-interaction is taken to be of the form

$$U(\sigma) = \frac{1}{3} b m_n \left(g_{\sigma N}\sigma\right)^3 + \frac{1}{4} c \left(g_{\sigma N}\sigma\right)^4. \tag{3}$$

The parameters of the model are the nucleon mass $M = 939$ MeV, the masses of mesons m_σ, m_ω, m_ρ and the coupling parameters.

The meson-hyperon couplings are assumed to be fixed fractions of the meson-nucleon couplings, $g_{iH} = x_{iH} g_{iN}$, where for each meson i, the values of x_{iH} are assumed equal for all hyperons H. The values of x_{iH} are chosen to reproduce the binding energy of the Λ at nuclear saturation as suggested in [16], and given in Table II.

From the Lagrangian density in Eq. (1), we obtain the following meson field equations in the mean-field approximation

$$m_\sigma^2 \sigma + \frac{\partial U(\sigma)}{\partial \sigma} = \sum_b g_{\sigma b} \rho_b^s = g_{\sigma N} \sum_b x_{\sigma b} \rho_b^s \tag{4}$$

$$m_\omega^2 \omega^0 = \sum_b g_{\omega b} \rho_b^v = g_{\omega N} \sum_b x_{\omega b} \rho_b^v \tag{5}$$

$$m_\rho^2 \rho^0 = \sum_b g_{\rho b} \tau_{3_b} \rho_b^v = g_{\rho N} \sum_b x_{\rho b} \tau_{3_b} \rho_b^v \tag{6}$$

where $\sigma = \langle\sigma\rangle$, $\omega^0 = \langle\omega^0\rangle$ and $\rho = \langle\rho^0\rangle$ are the nonvanishing expectation values of the mesons fields in uniform matter.

The Dirac equations for baryons and leptons are, respectively, given by

TABLE I: Static properties of baryons considered in this study. The mass, charge of baryon and strange charge of species b are denoted by m_b, q_b and q_s^b, respectively. The baryonic magnetic moment is denoted by μ_b. The baryonic AMM is given by $\kappa_b = (\mu_b/\mu_N - q_b m_p/m_b)$, where μ_N is the nuclear magneton.

b	m_b(MeV)	$q_b(e)$	q_s^b	μ_b/μ_N	κ_b
p	938.27	1	0	2.97	1.79
n	939.56	0	0	-1.91	-1.91
Λ^0	1115.7	0	-1	-0.61	-0.61
Σ^+	1189.4	1	-1	2.46	1.67
Σ^0	1192.6	0	-1	1.61	1.61
Σ^-	1197.4	-1	-1	-1.16	-038
Ξ^0	1314.8	0	-2	-1.25	-1.25
Ξ^-	1321.3	-1	-2	-0.65	0.06

$$\begin{aligned} \left[i\gamma_\mu\partial^\mu - q_b\gamma_\mu A^\mu - m_b^* - \gamma_0\left(g_\omega\omega^0 + g_\rho\tau_{3_b}\rho^0\right) - \frac{1}{2}\mu_N\kappa_b\sigma_{\mu\nu}F^{\mu\nu}\right]\Psi_b &= 0 \qquad (7)\\ \left(i\gamma_\mu\partial^\mu - q_l\gamma_\mu A^\mu - m_l\right)\psi_l &= 0 \qquad (8) \end{aligned}$$

where the effective baryon masses are given by

$$m_b^* = m_b - g_\sigma\sigma \qquad (9)$$

and ρ_b^s and ρ_b^v are the scalar number density and the vector number density, respectively. For charge-neutral, neutrino free, β-equilibrated matter, the following conditions are satisfied:

$$\begin{aligned} \mu_p &= \mu_{\Sigma^+} = \mu_n - \mu_e, \\ \mu_\Lambda &= \mu_{\Sigma^0} = \mu_{\Xi^0} = \mu_n, \\ \mu_{\Sigma^-} &= \mu_{\Xi^-} = \mu_n + \mu_e, \\ \mu_\mu &= \mu_e, \end{aligned} \qquad (10)$$

$$\sum_b q_b\rho_b^v + \sum_l q_l\rho_l^v = 0. \qquad (11)$$

The energy spectra for charged baryons, neutral baryons and leptons (electrons and muons) are, respectively, given by

$$\begin{aligned} E_{\nu,s}^b &= \sqrt{k_z^2 + \left(\sqrt{m_b^{*2} + 2\nu|q_b|B} - s\mu_N\kappa_b B\right)^2} + g_{\omega b}\omega^0 + \tau_{3_b}g_{\rho b}\rho^0 \qquad (12)\\ E_s^b &= \sqrt{k_z^2 + \left(\sqrt{m_b^{*2} + k_x^2 + k_y^2} - s\mu_N\kappa_b B\right)^2} + g_{\omega b}\omega^0 + \tau_{3_b}g_{\rho b}\rho^0 \qquad (13)\\ E_{\nu,s}^l &= \sqrt{k_z^2 + m_l^2 + 2\nu|q_l|B} \qquad (14) \end{aligned}$$

where $\nu = n + \frac{1}{2} - sgn(q)\frac{s}{2} = 0, 1, 2, \ldots$ enumerates the Landau levels (LL) of the fermions with electric charge q, the quantum number s is $+1$ for spin up and -1 for spin down cases.

For the charged baryons, we introduce the effective mass under the effect of a magnetic field

$$\bar{m}_b^c = \sqrt{m_b^{*2} + 2\nu|q_b|B} - s\mu_N\kappa_b B \qquad (15)$$

the expressions of the scalar and vector densities are, respectively, given by [6]

$$\rho_b^s = \frac{|q_b|Bm_b^*}{2\pi^2}\sum_{\nu=0}^{\nu\max}\sum_s \frac{\bar{m}_b^c}{\sqrt{m_b^{*2} + 2\nu|q_b|B}}\ln\left|\frac{k_{F,\nu,s}^b + E_F^b}{\bar{m}_b^c}\right|,$$

$$\rho_b^v = \frac{|q_b|B}{2\pi^2}\sum_{\nu=0}^{\nu\mathrm{max}}\sum_s k_{F,\nu,s}^b. \tag{16}$$

where $k_{F,\nu,s}^b$ is the Fermi momenta of charged baryon b with quantum numbers ν and s. The Fermi energy E_F^b is related to the Fermi momenta $k_{F,\nu,s}^b$ by

$$\left(k_{F,\nu,s}^b\right)^2 = \left(E_F^b\right)^2 - \left(\bar{m}_b^c\right)^2, \tag{17}$$

For the neutral baryons, there is no LL quantum number ν, so the Fermi momenta is denoted by $k_{F,s}^b$, and the Fermi energy E_F^b is given by

$$\left(k_{F,s}^b\right)^2 = \left(E_F^b\right)^2 - \bar{m}_b^2, \tag{18}$$

with

$$\bar{m}_b = m_b^* - s\mu_N\kappa_b B. \tag{19}$$

The scalar and vector densities of the neutral baryon b are, respectively, given by

$$\begin{aligned}\rho_b^s &= \frac{m_b^*}{4\pi^2}\sum_s\left[E_F^b k_{F,s}^b - \bar{m}_b^2\ln\left|\frac{k_{F,s}^b + E_F^b}{\bar{m}_b}\right|\right],\\ \rho_b^v &= \frac{1}{2\pi^2}\sum_s\left[\frac{1}{3}\left(k_{F,s}^b\right)^3 - \frac{1}{2}s\mu_N\kappa_b B\left(\bar{m}_b k_{F,s}^b + \left(E_F^b\right)^2\left(\arcsin\left(\frac{\bar{m}_b}{E_F^b}\right) - \frac{\pi}{2}\right)\right)\right].\end{aligned} \tag{20}$$

The vector density for leptons is given by

$$\rho_l^v = \frac{|q_l|B}{2\pi^2}\sum_{\nu=0}^{\nu\mathrm{max}}\sum_s k_{F,\nu,s}^l, \tag{21}$$

where $k_{F,\nu,s}^l$ is the lepton Fermi momenta, which is related to the Fermi energy E_F^l by

$$\left(k_{F,\nu,s}^l\right)^2 = \left(E_F^l\right)^2 - \bar{m}_l^2, \quad l = e, \mu, \tag{22}$$

with $\bar{m}_l^2 = m_l^2 + 2\nu|q_l|B$. The summation in ν in the above expressions terminates at ν_{max}, the largest value of ν for which the square of Fermi momenta of the particle is still positive and which corresponds to the closest integer from below defined by the ratio

$$\nu_{max} = \left[\frac{(E_F^l)^2 - m_l^2}{2|q_l|\,B}\right], \quad \text{leptons}$$

$$\nu_{max} = \left[\frac{(E_F^b + s\,\mu_N\;\kappa_b\,B)^2 - m_b^{*2}}{2|q_b|\,B}\right], \quad \text{charged baryons.}$$

The chemical potentials of baryons and leptons are defined as

$$\mu_b = E_F^b + g_{\omega b}\omega^0 + g_{\rho b}\tau_{3_b}\rho^0 \tag{23}$$

$$\mu_l = E_F^l = \sqrt{\left(k_{F,\nu,s}^l\right)^2 + m_l^2 + 2\nu|q_l|B}. \tag{24}$$

We solve the coupled Eqs. (4)-(11) self-consistently at a given baryon density $\rho = \sum_b \rho_b^v$ in the presence of strong magnetic fields. The energy density of neutron star matter is given by

$$\varepsilon_m = \sum_b \varepsilon_b + \sum_{l=e,\mu}\varepsilon_l + \frac{1}{2}m_\sigma^2\sigma^2 + U(\sigma) + \frac{1}{2}m_\omega^2\omega_0^2 + \frac{1}{2}m_\rho^2\rho_0^2, \tag{25}$$

where the energy densities of charged baryons ε_b^c, neutral baryons ε_b^n, and leptons ε_l have, respectively, the following forms

$$\begin{aligned}
\varepsilon_b^c &= \frac{|q_b|B}{4\pi^2}\sum_{\nu=0}^{\nu\max}\sum_s\left[k^b_{F,\nu,s}E^b_F+(\bar{m}^c_b)^2\ln\left|\frac{k^b_{F,\nu,s}+E^b_F}{\bar{m}^c_b}\right|\right], \\
\varepsilon_b^n &= \frac{1}{4\pi^2}\sum_s\left[\frac{1}{2}k^b_{F,s}\left(E^b_F\right)^3-\frac{2}{3}s\mu_N\kappa_b B\left(E^b_F\right)^3\left(\arcsin\left(\frac{\bar{m}_b}{E^b_F}\right)-\frac{\pi}{2}\right)\right. \\
&- \left.\left(\frac{1}{3}s\mu_N\kappa_b B+\frac{1}{4}\bar{m}_b\right)\left(\bar{m}_b k^b_{F,s}E^b_F+\bar{m}_b^3\ln\left|\frac{k^b_{F,s}+E^b_F}{\bar{m}_b}\right|\right)\right] \\
\varepsilon_l &= \frac{|q_l|B}{4\pi^2}\sum_{\nu=0}^{\nu\max}\sum_s\left[k^l_{F,\nu,s}E^l_F+\bar{m}_l^2\ln\left|\frac{k^l_{F,\nu,s}+E^l_F}{\bar{m}_l}\right|\right].
\end{aligned} \tag{26}$$

The pressure of neutron star matter is given by

$$P_m=\sum_i\mu_i\rho_i^v-\varepsilon_m=\mu_n\sum_b\rho_b^v-\varepsilon_m, \tag{27}$$

where the charge neutrality and β-equilibrium conditions are used to get the last equality. The total energy density and the total pressure of the system are given, by adding the corresponding contribution of the magnetic field,

$$\begin{aligned}
\varepsilon &= \varepsilon_m+\frac{B^2}{2}, \\
P &= P_m+\frac{B^2}{2}.
\end{aligned} \tag{28}$$

III. QUARK MATTER EQUATIONS OF STATE

The MIT Bag model has been extensively used to describe quark matter. In its simplest form, the quarks are considered to be free inside a Bag and the thermodynamic properties are derived from the Fermi gas model. In the presence of a strong magnetic field Eqs. (28) are still valid with the energy density and pressure of quark stellar matter, and quark density, respectively, given by

$$\begin{aligned}
\varepsilon_m &= \sum_{i=u,d,s,e}\left\{\frac{|q_i|B}{4\pi^2}\sum_{\nu=0}^{\nu^i_{max}}g_i\left[\mu_i\sqrt{\mu_i^2-\left(M^{(i)}_\nu\right)^2}+\left(M^{(i)}_\nu\right)^2\ln\left|\frac{\mu_i+\sqrt{\mu_i^2-\left(M^{(i)}_\nu\right)^2}}{\left(M^{(i)}_\nu\right)^2}\right|\right]\right\}+\text{Bag}, \\
P_m &= \sum_{i=u,d,s,e}\left\{\frac{|q_i|B}{4\pi^2}\sum_{\nu=0}^{\nu^i_{max}}g_i\left[\mu_i\sqrt{\mu_i^2-\left(M^{(i)}_\nu\right)^2}-\left(M^{(i)}_\nu\right)^2\ln\left|\frac{\mu_i+\sqrt{\mu_i^2-\left(M^{(i)}_\nu\right)^2}}{\left(M^{(i)}_\nu\right)^2}\right|\right]\right\}-\text{Bag}, \\
\rho_q &= \sum_{i=u,d,s}\left\{\frac{|q_i|B}{2\pi^2}\sum_{\nu=0}^{\nu^i_{max}}g_i\sqrt{\mu_i^2-\left(M^{(i)}_\nu\right)^2}\right\},
\end{aligned} \tag{29}$$

where $M^{(i)}_\nu=\sqrt{m_i^2+2\nu|q_i|B}$ and ν runs over the allowed LL, g_i denotes the degeneracy of the i-th species, *i.e.*, six for the quarks and two for the leptons, m_q the quarks masses and Bag represents the bag pressure.

We use $m_u=m_d=5.5$MeV, $m_s=150.0$MeV and two values for the Bag $(165\text{MeV})^4$ and $(180\text{MeV})^4$. In what follows, the baryon density ρ is defined as $\rho=\sum_q\rho_q/3$.

In a star with quark matter we must impose both beta equilibrium and charge neutrality. For β-equilibrium matter we must add the contribution of the leptons as free Fermi gases (electrons and muons) to the energy density, pressure and entropy density. The relations between the chemical potentials of the different particles are given by

$$\mu_s=\mu_d=\mu_u+\mu_e,\quad \mu_e=\mu_\mu. \tag{30}$$

In terms of neutron and electric charge chemical potentials μ_n and μ_e, one has

$$\mu_u = \frac{1}{3}\mu_n - \frac{2}{3}\mu_e, \text{ and } \mu_s = \mu_d = \frac{1}{3}\mu_n + \frac{1}{3}\mu_e. \tag{31}$$

For the charge neutrality we impose

$$\rho_e + \rho_\mu = \frac{1}{3}\left(2\rho_u - \rho_d - \rho_s\right). \tag{32}$$

IV. MIXED PHASE AND HYBRID STAR PROPERTIES

We study the hadron-quark phase transition which may occur in the core of massive neutron stars. We will use the Gibbs criteria and global charge conservation to describe the mixed phase of hadronic and quark matter [13], which for two conserved charges, the electric charge and the baryonic charge, are given by

$$\begin{aligned} \mu_{\mathrm{HP},i} = \mu_{\mathrm{QP},i} &= \mu_i, \ i = n, e, \\ P_{\mathrm{HP}}\left(\mu_{\mathrm{HP}}\right) &= P_{\mathrm{QP}}\left(\mu_{\mathrm{QP}}\right). \end{aligned} \tag{33}$$

where the subscripts HP and QP denote, respectively, the hadronic and the quark phase. Imposing the condition of global conservation of the electric and baryonic charges, *i.e*, both hadronic and quark matter are allowed to be separately charged and have different baryonic densities. We impose

$$\begin{aligned} \chi\rho_c^{\mathrm{QP}} + (1-\chi)\,\rho_c^{\mathrm{HP}} + \rho_c^l &= 0, \\ \chi\rho^{\mathrm{QP}} + (1-\chi)\,\rho^{\mathrm{HP}} &= \rho \end{aligned} \tag{34}$$

where χ is the volume fraction occupied by the quark phase and $(1-\chi)$ the volume fraction occupied by the hadron phase, ρ_c^i (ρ^i) are the electric (baryonic) charge densities of quark and hadron phases and ρ_c^l is the lepton electric charge density. The total energy density in the mixed phase reads

$$\varepsilon = \chi\varepsilon^{\mathrm{QP}} + (1-\chi)\,\varepsilon^{\mathrm{HP}} + \varepsilon_l. \tag{35}$$

The mixed phase is charactrized by a value of χ which varies between 0, at the onset of the mixed phase, and 1, at the onset of the quark matter. The baryonic densities ρ_1 and ρ_2 given in Tables III and IV, correspond, respectively, to $\chi = 0$ and $\chi = 1$ and define the onset of the mixed phase (ρ_1) and the onset of the quark phase (ρ_2). The mixed phase is determined by simultaneously imposing the Gibbs conditions (33), charge conservation conditions (34), chemical equilibrium conditions (10), (11), (31) and (32), and the field equations (4-8).

However, we should point out that the Gibbs construction is an approximation that although taking correctly into account the existence of two charge conserving conditions does not take into account surface effects and the Coulomb field [17, 18]. A complete treatment of the mixed phase requires the knowledge of the surface tension between the two phases which is not well established and may have a value between 10-100 MeV/fm^2 [18]. The Gibbs construction gives results close to the ones obtained with the lower value of the above surface tension range, and is recovered for a zero surface tension. We could have also considered the Maxwell construction, for which only baryon number conservation is considered, *i. e.* the first condition of Eq. (33) is only satisfied for $i = n$. It has been shown in [18] that the Maxwell description of the mixed phase gives a good description if the surface tension is very large. Therefore, for comparison we will also determine the mixed phase using a Maxwell construction, see Tables V and VI.

The EOS for the mixed phase are then constructed. Consequently, we can compute the properties of the neutron star. In the present study we consider very strong magnetic fields which have a contribution to the total pressure at least as large as the contribution coming from matter. This means that stars with non-spherical configurations should be considered [15, 19]. We will, however, consider spherical stars and use the Tolman-Oppenheimer-Volkoff (TOV) equations for the structure of a static, spherically symmetric star to obtain the mass-radius (M-R) relation of neutron star. With this approximation our results and, therefore, conclusions should be taken with care.

V. RESULTS AND DISCUSSION

In order to study the effect of strong magnetic fields on the structure of neutron star we use the GM1 parametrisation of the NLW model given in Table. II, [16]. Since, to date, there is no information available on the interior magnetic field of the star, we will assume that the magnetic field is baryon density-dependent as suggested by Ref. [14]. The variation

TABLE II: The parameter set GM1 [16]used in the calculation.

ρ_0 (fm^{-3})	-B/A (MeV)	M^*/M	$g_{\sigma N}/m_\sigma$ (fm)	$g_{\omega N}/m_\omega$ (fm)	$g_{\rho N}/m_\rho$ (fm)	$x_{\sigma H}$	$x_{\omega H}$	$x_{\rho H}$	b	c
0.153	16.30	0.70	3.434	2.674	2.100	0.600	0.653	0.600	0.002947	-0.001070

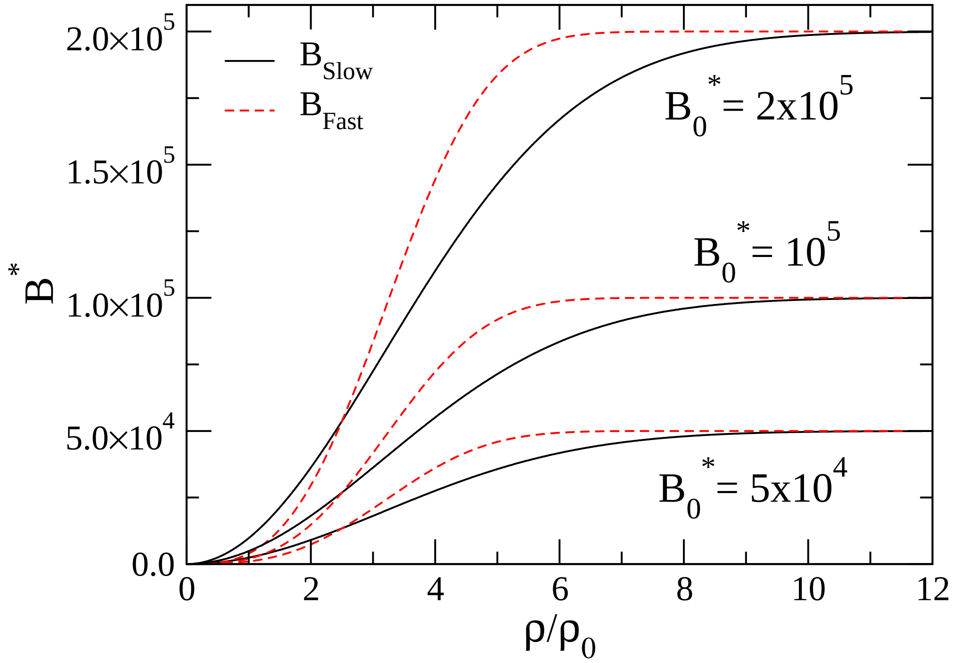

FIG. 1: (Color online). The magnetic field B defined in (36) as function of the baryonic density for several values of the parameter B_0 and for the slow ($\beta = 0.05$ and $\gamma = 2$), and fast parametrisations ($\beta = 0.02$ and $\gamma = 3$).

of the magnetic field B with the baryons density ρ from the center to the surface of a star is parametrized [14, 20] by the following form

$$B\left(\frac{\rho}{\rho_0}\right) = B^{\text{surf}} + B_0\left[1 - \exp\left\{-\beta\left(\frac{\rho}{\rho_0}\right)^{\gamma}\right\}\right], \tag{36}$$

where ρ_0 is the saturation density, B^{surf} is the magnetic field at the surface taken equal to 10^{15}G in accordance with the values inferred from observations and B_0 represents the magnetic field for large densities. The parameters β and γ are chosen in such way that the field decreases fast or slow with the density from the centre to the surface. In this work, we will use two sets of values: a slowly varying field with $\beta = 0.05$ and $\gamma = 2$, and a fast varying one defined by $\beta = 0.02$ and $\gamma = 3$. We give the magnetic field in units of the critical field $B_e^c = 4.414 \times 10^{13}$ G, so that $B = B^*\, B_e^c$. We further take B_0^* as a free parameter to check the effect of different fields.

In Fig.1 we plot the variation of the magnetic field, for the two parametrisations of the magnetic field as function of the baryonic density for several values of the parameter B_0^* in Eq. (36). For the slowly varying field the magnitude B_0^* is reached for densities $\rho > 10\rho_0$, where ρ_0 is the saturation density, while for the fast changing field this value is reached for $\rho > 5\rho_0$. On the other hand, for densities $\rho < 3\rho_0$ the slowly varying magnetic field is stronger. This fact will influence the stiffness of the equation of state (EOS): the EOS is stiffer a) at low densities if a slowly varying field is considered; b) at high densities if a fast varying field is chosen. We present the numerical results for the slowly and fast parametrisations of the density-dependent magnetic field and for two Bag constants $(180\text{MeV})^4$ and $(165\text{MeV})^4$. In all figures where both cases are considered we show on the left panel the results for $\text{Bag}^{1/4}$ =180 MeV and on the right panel the results for and $\text{Bag}^{1/4}$=165 MeV. Furthermore, in all the figures, we will only show results obtained without the inclusion of the baryonic AMM's, because for the intensity of the magnetic fields considered the

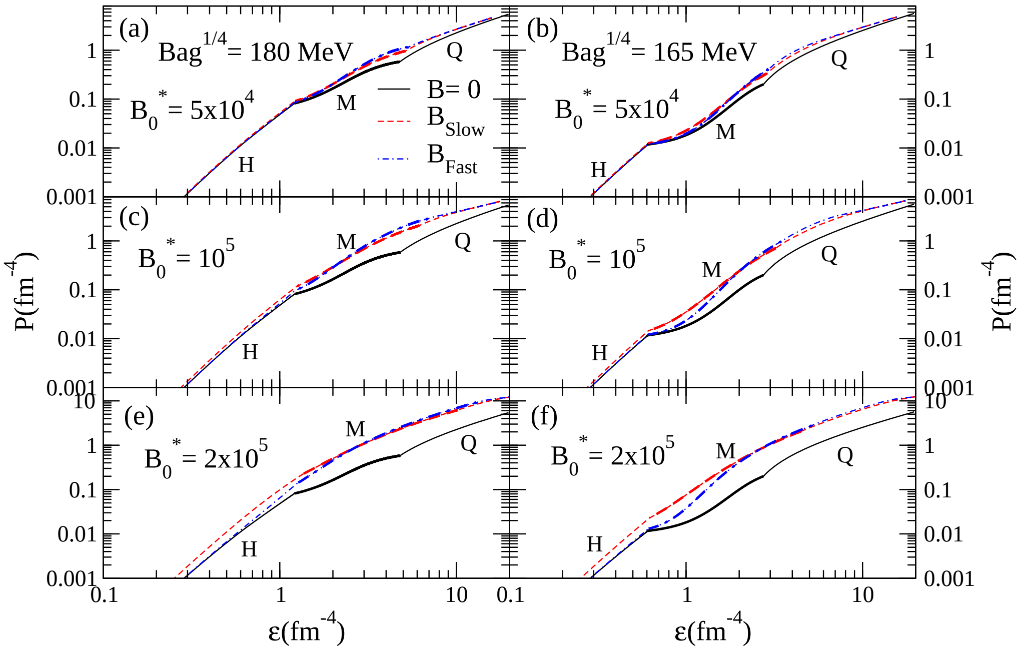

FIG. 2: (Color online). EOS for stellar matter for GM1 and for several values of the magnetic field identified by the B_0 parameter of Eq. (36). In the left panel (a), (c), and (e) for Bag$^{1/4}$=180 MeV and in the right panel (b), (d), and (f) for Bag$^{1/4}$=165 MeV. In each figure we include the $B = 0$ EOS, for reference, and the EOS obtained with the slow and fast parametrisation of Eq. (36). The hadron, mixed and quark phases are identified, respectevely, by a H, a M and thick lines, and a Q.

contribution to the EOS is negligible. The effect of the AMM is non negligible for $B^* > 10^5$ [6] but, as it will be shown later in this section at the centre of the stars described in the present work these values will never be reached. In Fig. 2, we plot the EOS of neutron stellar matter, for the two parametrisations of the magnetic field, defined by Eqs. (28). For comparison we include in all figures the EOS for $B = 0$. The hadron phase is identified with a H (left part of the curves), the mixed phase is plotted with thick lines and identified with a M and the quark phase is identified with a Q (right part of the curves). We point out that these curves include both the contribution of stellar matter and the contribution of the magnetic field in the energy density and the pressure. In Fig. 3 we plot only the pressure term coming from the stellar matter contribution, Eq. (27), as a function of the baryonic density for the largest $B_0^* = 2 \times 10^5$ in order to clearly show the effect of the magnetic field on the stellar matter contribution to the total EOS. We also plot, seperatly, the contribution of the magnetic field (thin line), which allows us to identify at which density the magnetic field contribution becomes larger than the matter contribution. The vertical lines identify the central density of the maxinmum mass star for both parameters bag considered. Figs. 2 and 3 are completed with Tables III and IV, where for the two parametrisations of the magnetic fields and, respectively, for Bag$^{1/4}$=180 MeV and Bag$^{1/4}$=165 MeV, the mixed phase density boundaries and the corresponding total energy densities defined in Eq. (28) are given for several values of the magnetic field. The onset of the mixed phase occurs at density ρ_1, and the pure quark phase begins at density ρ_2. In Tables V and VI we give, for comparison, the same quantities obtained using the Maxwell construction. Independently of the magnetic field, the onset of the mixed phase and quark pure phase occurs at lower densities for the smaller value of bag pressure [21], because the EOS is much stiffer for Bag$^{1/4}$ = 180 MeV than Bag$^{1/4}$ = 165 MeV.

We now discuss the effect of the presence of a strong magnetic field with magnitude $B_0^* = 5 \times 10^4$, 10^5, and 2×10^5 ($\sim 10^{18} - 10^{19}$ G) on the equation of state (EOS). The main conclusions are: a) the presence of the field does not affect the baryonic density at the onset of the mixed phase because the intensity of the field is too low ($B^* < 2 \times 10^4$); b) the baryonic density at the onset of the pure quark matter decreases with the increase of the magnetic field, as seen in Fig. 3 and discussed in Ref. [14]. This is due to the fact that the EOS of quark matter under a strong magnetic field becomes softer. The softening of the quark EOS with the increase of the magnetic field has been obtained with

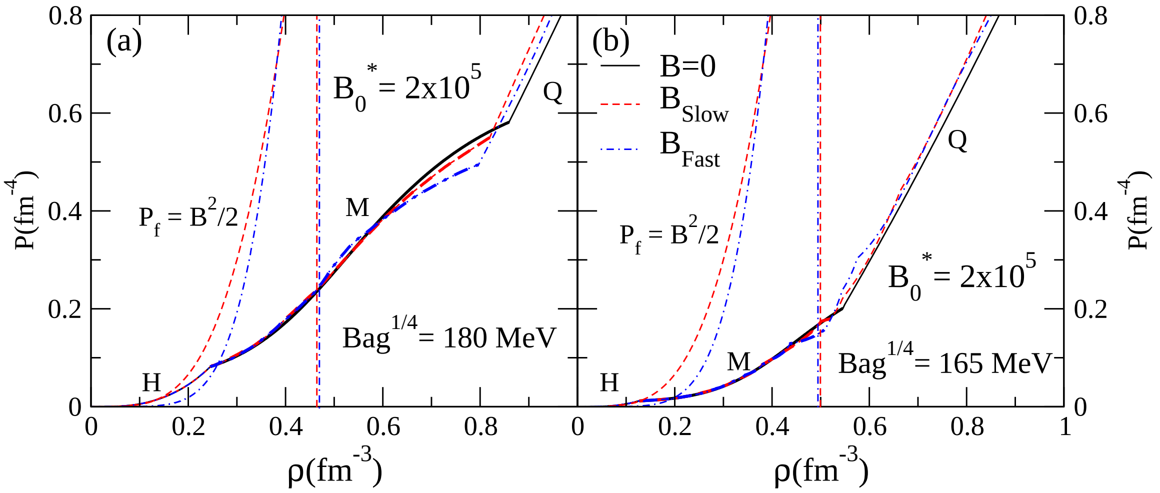

FIG. 3: (Color online). EOS for stellar matter for GM1 and for $B_0^* = 2 \times 10^5$. In the left panel (a) for Bag$^{1/4}$=180 MeV and in the right panel (b) for Bag$^{1/4}$=165 MeV. In each figure we include the $B = 0$ EOS, for reference, and the EOS obtained with the slow and fast parametrisation of Eq. (36). The vertical lines identify the central baryonic density of the stable star with maximum mass.

TABLE III: The phase density boundaries, the onset of the mixed phase $u_1 = \rho_1/\rho_0$ and the onset of the pure quark phase $u_2 = \rho_2/\rho_0$, and the corresponding total energy densities, for several values of magnetic field using the two parametrisations defined in Eq. (36) (slow and fast). The bag constant is Bag$^{1/4}$=180 MeV, and the nuclear matter saturation density $\rho_0 = 0.153$ fm^{-3} for GM1 model.

B_0^*		$u_1 = \rho_1/\rho_0$	$\varepsilon_1(\text{fm}^{-4})$	$u_2 = \rho_2/\rho_0$	$\varepsilon_2(\text{fm}^{-4})$
$B = 0$		1.605	1.212	5.618	4.794
$B_0^* = 5 \times 10^4$	slow	1.604	1.220	5.588	5.145
	fast	1.606	1.218	5.583	5.333
$B_0^* = 10^5$	slow	1.609	1.252	5.510	6.175
	fast	1.605	1.228	5.477	6.914
$B_0^* = 2 \times 10^5$	slow	1.614	1.366	5.357	10.198
	fast	1.603	1.273	5.206	13.017

other quark models like the Nambu-Jona Lasinio (NJL) model [12, 22]; c) due to the magnetic field contribution to the pressure and energy density, Eqs. (28) , the extension of the mixed phase in terms of the energy density increases, as can be seen from Tables III and IV and from Fig. 2, mainly, shifting the onset of the quark phase to higher energy densities; d) the contribution of the magnetic field makes the total EOS harder. However, the slow and fast parametrisations have different effects. At low densities the soft parametrisation correponds to a stronger magnetic field and therefore gives rise to a harder EOS in that range of densities and favours the onset of the mixed phase at larger energy densities. In Tables III and IV ε_1 is larger for the slow paramerisation. On the other hand, for large densities the fast parametrisation corresponds to larger magnetic fields and a harder EOS. The onset of the quark phase occurs at larger energy densities, *i.e.* for a given B_0^* value, ε_2 is larger for the fast parametrisation; e) the transition to the mixed phase is less affected by the magnetic field than the transtion to a pure quark matter. This is due to the magnetic field parametrisation, (36), which gives a weaker magnetic field at the baryonic densities of the mixed phase onset. On the other hand, the transition to a pure quark phase is strongly affected because for the densities at which it occurs the magnetic field is stronger, more than 50% (75%) its maximum value for the slow (fast) varying magnetic field; f) for all values of the magnetic field considered, the extension of the mixed-phase is larger for the larger bag pressure due to the larger stiffness of the quark phase EOS. From Tables V and VI, for the Maxwell construction similar conclusions are drawn, however with a larger baryonic density at the onset of the mixed phase, $\sim \rho_0$ larger for Bag$^{1/4}$=180 MeV and $\sim 0.5\rho_0$ larger for Bag$^{1/4}$=165 MeV, and a smaller one at the on set of the pure quark phase, $\sim \rho_0$ smaller for Bag$^{1/4}$=180 MeV and $\sim 0.5\rho_0$ smaller for Bag$^{1/4}$=165 MeV.

In Ref. [14] the magnetic field contribution was also taken into account in the EOS used to integrate the TOV equations, however this term enters with the wrong sign in the total pressure, it gives a negative contribution, and therefore, the EOS becomes very soft for strong magnetic fields and the formation of very massive stars is not allowed.

TABLE IV: Same as Table III, but for Bag$^{1/4}$=165 MeV.

B_0^*		$u_1 = \rho_1/\rho_0$	$\varepsilon_1(\mathrm{fm}^{-4})$	$u_2 = \rho_2/\rho_0$	$\varepsilon_2(\mathrm{fm}^{-4})$
$B = 0$		0.832	0.613	3.567	2.748
$B_0^* = 5 \times 10^4$	slow	0.831	0.613	3.546	2.869
	fast	0.831	0.612	3.538	2.940
$B_0^* = 10^5$	slow	0.830	0.614	3.519	3.232
	fast	0.831	0.612	3.478	3.467
$B_0^* = 2 \times 10^5$	slow	0.830	0.623	3.402	4.496
	fast	0.832	0.614	3.317	5.162

TABLE V: The phase density boundaries obtained with Maxwell construction, the onset of the mixed phase $u_1 = \rho_1/\rho_0$ and the onset of the pure quark phase $u_2 = \rho_2/\rho_0$, and the corresponding total energy densities, for several values of magnetic field using the two parametrisations defined in Eq. (36) (slow and fast). The bag constant is Bag$^{1/4}$=180 MeV, and the nuclear matter saturation density $\rho_0 = 0.153$ fm^{-3} for GM1 model.

B_0^*		$u_1 = \rho_1/\rho_0$	$\varepsilon_1(\mathrm{fm}^{-4})$	$u_2 = \rho_2/\rho_0$	$\varepsilon_2(\mathrm{fm}^{-4})$
$B = 0$		2.819	2.250	4.606	3.855
$B_0^* = 5 \times 10^4$	slow	2.799	2.297	4.580	4.089
	fast	2.787	2.297	4.580	4.275
$B_0^* = 10^5$	slow	2.706	2.379	4.510	4.760
	fast	2.715	2.422	4.471	5.420
$B_0^* = 2 \times 10^5$	slow	2.477	2.628	4.228	6.918
	fast	2.475	2.612	4.314	9.813

TABLE VI: Same as Table V, but for Bag$^{1/4}$=165 MeV.

B_0^*		$u_1 = \rho_1/\rho_0$	$\varepsilon_1(\mathrm{fm}^{-4})$	$u_2 = \rho_2/\rho_0$	$\varepsilon_2(\mathrm{fm}^{-4})$
$B = 0$		1.283	0.958	2.922	2.235
$B_0^* = 5 \times 10^4$	slow	1.276	0.956	2.933	2.318
	fast	1.276	0.953	2.933	2.339
$B_0^* = 10^5$	slow	1.260	0.954	2.918	2.524
	fast	1.255	0.939	2.902	2.583
$B_0^* = 2 \times 10^5$	slow	1.206	0.946	2.878	3.321
	fast	1.196	0.901	2.847	3.507

As already discussed in Ref. [21], the presence of strangeness in the core of a neutron stars will affect some of their properties. In Fig. 4 we show the strangeness fraction defined by :

$$\mathfrak{r}_s = \chi \mathfrak{r}_s^{QP} + (1-\chi)\mathfrak{r}_s^{HP} \tag{37}$$

with,

$$\mathfrak{r}_s^{QP} = \frac{\rho_s}{3\rho}, \qquad \mathfrak{r}_s^{HP} = \frac{\sum_b \left|q_s^b\right| \rho_b}{3\rho} \tag{38}$$

where ρ_s is the strange quark density, and q_s^b is the strange charge of baryon b, listed in Table I.

Only the strongest field considered affects considerably the strangeness fraction. At the onset of the pure quark phase, the strange quark fraction has reached 30% of the baryonic matter. Although the fraction of strangeness varies in the mixed-phase, it has almost the same value in the quark phase. For $B_0^* = 2 \times 10^5$, with both bag values and with the two parametrisations of the magnetic field used the effect of the Landau quantisation appears, and the strangeness fraction obtained is slightly oscillating around the $B = 0$ result. The strangeness content increases slightly faster at larger densities with the fast parametrisation. The presence of this strong magnetic field shifts to lower densities the onset of the 30% fraction of strange matter, corresponding to the onset of the quark phase. The thin vertical lines included in the Fig. 4 identifies the central baryonic density of the maximum mass star. For Bag$^{1/4}$=180 MeV the strangeness fraction at given density is never larger than 15%, while for Bag$^{1/4}$=165 MeV it can be as large as 30%.

TABLE VII: Properties of the stable hybrid star with maximum mass, for Bag$^{1/4}$=180 MeV and for several values of magnetic field using [see Eq. (36)] with the slow and fast parametrisations. M_{max}, M^b_{max}, R, E_0, ρ^c, and B^*_c are, respectively, the gravitational and baryonic masses, the star radius, the central energy density, the central baryonic density, and the value of the magnetic field at the centre.

B^*_0		$M_{max}[M_\odot]$	$M^b_{max}[M_\odot]$	R [km]	$E_0[\text{fm}^{-4}]$	$u^c = \rho^c/\rho_0$	B^*_c
$B = 0$		1.42	1.57	10.22	8.05	8.680	
$B^*_0 = 5 \times 10^4$	slow	1.74	1.93	11.56	5.75	6.150	4.248×10^4
	fast	1.85	2.06	11.49	5.85	6.092	4.948×10^4
$B^*_0 = 10^5$	slow	2.23	2.48	12.35	5.23	4.843	6.908×10^4
	fast	2.33	2.55	11.88	5.62	4.595	8.565×10^4
$B^*_0 = 2 \times 10^5$	slow	2.86	3.12	14.39	3.73	3.033	7.375×10^4
	fast	2.76	2.88	13.15	4.41	3.092	8.926×10^4

TABLE VIII: Same as Table VII, but for Bag$^{1/4}$=165 MeV.

B^*_0		$M_{max}[M_\odot]$	$M^b_{max}[M_\odot]$	R [km]	$E_0[\text{fm}^{-4}]$	$u^c = \rho^c/\rho_0$	B^*_c
$B = 0$		1.47	1.68	8.86	10.02	10.673	
$B^*_0 = 5 \times 10^4$	slow	1.72	1.95	9.80	8.24	8.588	4.877×10^4
	fast	1.81	2.04	10.07	7.55	7.928	5.000×10^4
$B^*_0 = 10^5$	slow	2.14	2.36	11.07	6.52	5.902	8.251×10^4
	fast	2.26	2.45	11.01	6.36	5.203	9.404×10^4
$B^*_0 = 2 \times 10^5$	slow	2.73	2.93	13.55	4.23	3.294	8.377×10^4
	fast	2.68	2.78	12.50	4.80	3.222	9.759×10^4

We next study the effect of the magnetic field on the properties of the stars described by the EOS discussed above. We will consider that the stars have spherical symmetry. The maximum gravitational and baryonic masses of the

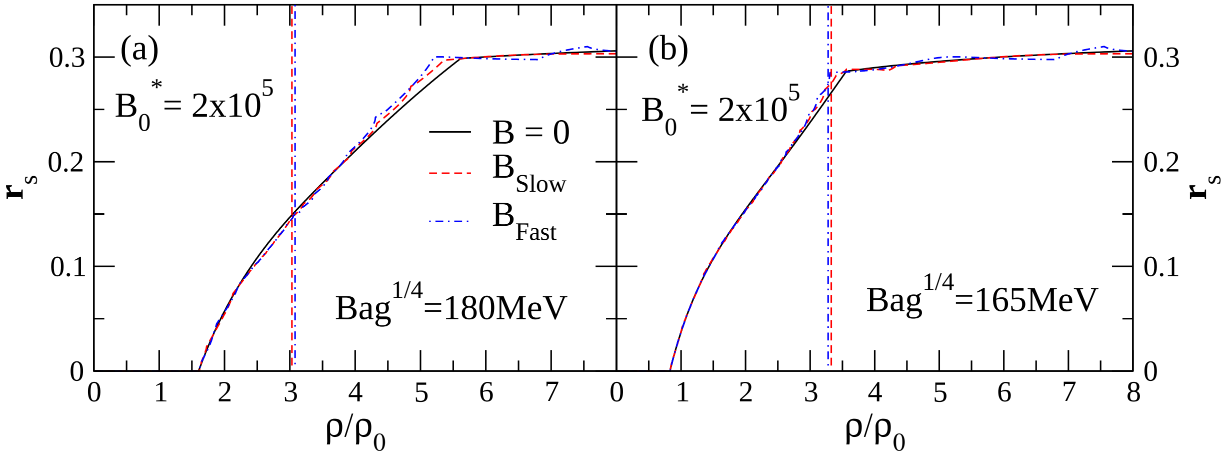

FIG. 4: (Color online). Strangeness fraction, defined in Eq. (37), as function of the baryonic density, for $B^*_0 = 2 \times 10^5$ in the interior of the star, (a) for Bag$^{1/4}$=180 MeV and (b) for Bag$^{1/4}$=165 MeV. The vertical lines identify the central baryonic density of the stable star with maximum mass.

stable stars, radius, central energy density, and central baryonic density, and the corresponding magnetic field at the centre of the star, obtained by solving the Tolman-Oppenheimer-Volkoff equation, are given for Bag$^{1/4}$=180 MeV and Bag$^{1/4}$=165 MeV in Tables VII and VIII, respectively. We note that the central energy and baryonic densities are decreasing when the magnetic field increases, while the maximum masses and the corresponding radius increase with the magnetic field, contrary to the results of [14] where the magnetic field contribution has entered with the wrong sign in the total pressure expression, giving rise to very soft EOS for large fields. This behavior is due to the stiffening of the EOS with the magnetic field. In the cases under study the magnetic field at the center of the maximum mass configuration is never larger than 4×10^{18} G a value close to the limit obtained from the virial theorem.

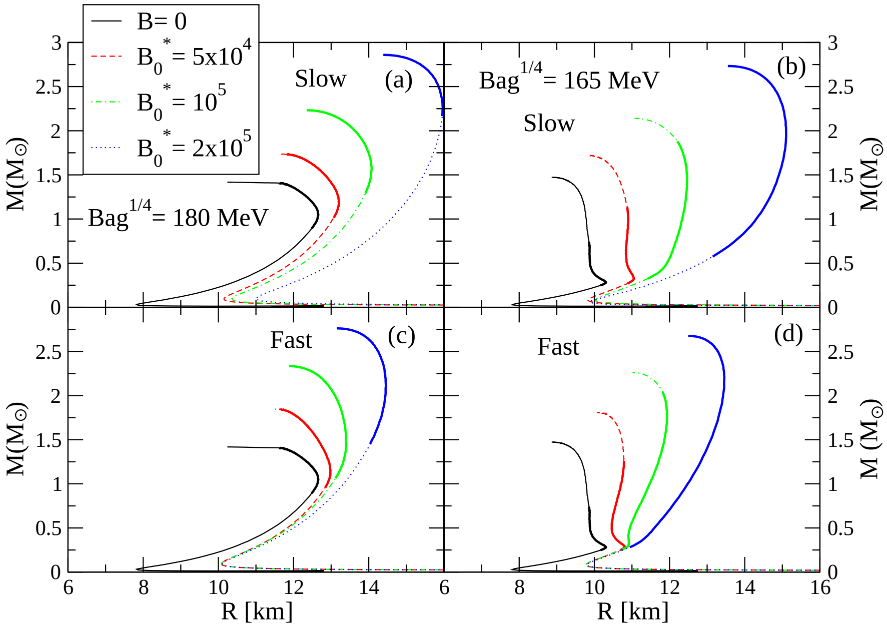

FIG. 5: (Color online). Mass-radius relation of the hybrid stars described in the present work for several values of magnetic field using the slow and fast varying parametrisations of B. (a) and (c) for Bag$^{1/4}$=180 MeV, and (b) and (d) for Bag$^{1/4}$=165 MeV. The thick lines identify the stars with a mixed phase at the center. Stars with smaller masses are hadronic stars with no quark matter, and stars with larger masses have a pure quark core. For the $B_0^* = 2 \times 10^5$ there are no stars with a quark core.

The mass/radius curves for the families of stars corresponding to the maximum mass configurations given in Tables VII and VIII are plotted in Fig. 5. The thick lines correspond to stars for which the central density lies within the mixed phase. For the largest bag pressure there is a quark core only for the no field configuration and the smallest field considered. For the smallest bag pressure only the strongest field considered gives rise to a no quark core configuration. It is interesting to notice the strong effect of the magnetic field parametrisation on the corresponding family star properties. For the stars that have no quark phase in their interior the central density is always smaller than $\rho \sim 2.5\rho_0$ for which the slow and the fast varying parametrisations give the same magnetic field magnitude, see Fig. 1. Below this density the slowly varying parametrisation gives rise to larger magnetic fields and therefore to a harder EOS. The corresponding stars have larger radius and larger masses due to the larger incompressibility modulus. This explains why the maximum radius of stars with more than 0.5 $M_\odot$ is larger for the slowly varying field. This difference can be as large as 1 km for the largest field considered.

However, the largest mass configuration is obtained for central magnetic fields larger for the fast varying field and therefore, the maximum mass is larger in this case, except for the largest central value of the magnetic field considered. For this value, the central density for the maximum mass configuration is $\sim 3 - 3.3\,\rho_0$. From Fig. 1 it is clear that these densities are just above the critical density values for which both parametizations give the same magnetic field and, therefore, the star obtained with the slowly varying parametrisation has, for most of the densities a larger field. The size of the star is largely influenced by the lower density layers and therefore most of the maximum mass stars have a larger radius for the slowly varying field, which give rise to larger magnetic fields in the low density layers.

For a central magnetic field $\sim 3 \times 10^{18}$ G we get maximum mass configuration with a mass 2.2-2.3 $M_\odot$. Slightly larger central fields predict even more massive stars with $M > 2.7\,M_\odot$. These values would be able to describe highly massive compact stars, such as the one associated to the millisecond pulsars PSR B1516 + 02B [23], and the one in PSR J1748-2021B [24] in case they are confirmed. Otherwise an upper limit on the possible magnitude of the magnetic field at the center of a compact star may be obtained.

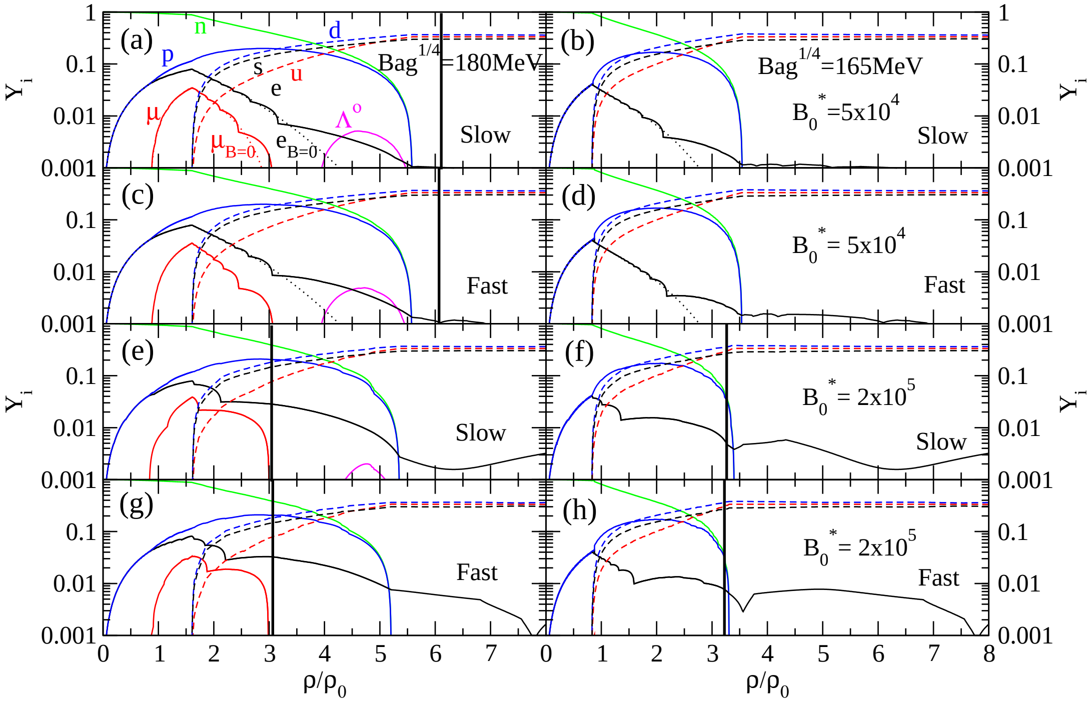

FIG. 6: (Color online). Particle fractions $Y_i = \rho_i/\rho$ as function of ρ/ρ_0, for i=baryons, leptons, and quarks, for two values of the magnetic field ($B_0^* = 5\times10^4$ (a)-(d), and $B_0^* = 2\times10^5$ (e)-(h)), with both parametrisations (slow and fast). We have considered two bag pressures: Bag$^{1/4}$=180 MeV for (a), (c), (e), and (g) figures, and Bag$^{1/4}$=165 MeV for (b), (d), (f), and (h) figures. The vertical lines represent the density ρ^c at the center of the star with maximum mass.

The properties of the stars are strongly influenced by the magnitude of the magnetic field in their interior and the characteristics of the hadronic EOS become less important the larger the field is. It is also clear that a quark phase is not favoured if a strong magnetic field exists in the interior of the star. This conclusion is based on the Gibbs construction of the mixed phase. Within a Maxwell construction, the onset of pure quark matter occurs at smaller densities and, therefore, a small quark core could still exist for the smaller Bag constant.

We have also looked at the baryonic and leptonic composition of the stars. In Fig. 6 we plot the lepton, baryon and the quark abundances. We only show the particle fractions for the smallest and the largest magnetic fields considered in the present work. The vertical lines in the figures represent the central density of the configuration with maximum mass when it lies within the range of densities shown. Large magnetic fields prevent the appearance of a quark phase, enhance the leptonic fraction and reduce slightly the mixed phase baryonic density extention. For strong magnetic fields, stars are mainly hadronic even when we consider a soft quark EOS. We also conclude that the only effect of the slow/fast varying magnetic field is the appearance at low/high densities of a larger leptonic fraction. The contribution of hyperons is minimal or even zero.

VI. CONCLUSIONS

We have studied the influence of a static magnetic field on the deconfinement phase transition in the interior of a compact star. For the hadronic phase we took the GM1 parametrisation of the NLWM [16] and for the quark phase the MIT bag model with two different bag pressures, one corresponding to a soft and the other to a hard quark EOS. The mixed phase was built imposing the Gibbs conditions [13]. It was considered that the magnitude of the magnetic field increases with density from a surface field of the order of 10^{15} G to a central field $\sim 5 \times 10^{18}$G, and both a fast and a slow changing field were used.

It was shown that due to the weakness of the magnetic field at low densities, the onset of the mixed phase is not affected by the magnetic field. The baryonic density at the onset of the pure quark phase is only slightly reduced for the magnetic fields considered, but, due to the contribution of the magnetic field to the total pressure and total energy density, the EOS of stellar matter in the presence of a strong magnetic field becomes much harder and the mixed phases extends to larger energy density ranges. As a consequence, the family of stars corresponding to these EOS have configurations with larger masses and radius. It was shown that the density dependence of the magnetic field will influence the star properties, with a slowly increasing field giving rise to larger radius.

Due to the magnetic field pressure, the quark phase is not favoured, and stars with strong magnetic field are mainly hadronic with very small hyperon contributions. Stars with very high masses and radius are predicted and maximum masses of observed compact stars may set an upper limit of the largest possible magnetic field at the center of the star, $\sim 2 \times 10^{18}$ G for 2 $M_\odot$ stars.

In the present work we have not taken into account the possibility of color superconductivity (CS) which was shown to be important to describe the groundstate of quark matter at high chemical potential and low temperature (for a review see [25]). In particular, the effect of CS, in a color-flavor locked (CFL) phase, on the structure of hybrid stars was discussed in Ref. [26]. Moreover, it has already been studied the effect of strong magnetic fields on the CS properties which can be drastic, [27]. However, we point out that although a strong magnetic field may have important effects on the stellar quark matter EOS the contribution of the magnetic field energy to the total energy of the star will impose severe restrictions on the maximum field a star may support and on the baryonic density reached at the centre of the star, [15]. In the present work, we have shown that: for very strong magnetic fields the central core of the star will probably never be in a quark phase, but at most in a mixed phase.

Very strong magnetic fields can only occur in very young compact stars before the magnetic field has decayed [28]. We may therefore conclude that, not only neutrino trapping in the protoneutron star phase [29], but also a very strong magnetic field in the interior of a compact star strongly precludes the formation of a quark phase. Quark matter thermal nucleation in hot and dense hadronic matter has been proposed by several authors [30]. In these studies, it was found that the prompt formation of a critical size drop of quark matter via thermal activation is possible above a temperature of about $2-3$ MeV, and as a consequence, it was inferred that pure hadronic stars are converted to hybrid stars or quark stars within the first seconds after their birth. The presence of a strong magnetic field would make this scenario less probable.

Acknowledgments

This work was partially supported by FEDER and Projects PTDC/FP/64707/2006 and CERN/FP/83505/2008, and by COMPSTAR, an ESF Research Networking Programme.

---

[1] R. C. Duncan and C. Thompson, Astronphys. J. **392**, L9 (1992).
[2] V. V. Usov, Nature 357, 472 (1992).
[3] B. Paczyński, Acta Astron. 42, 145 (1992).
[4] S. L. Shapiro and S. A. Teukolsky, *Black holes, white dwarfs and neutron stars*, Wiley-interscience New York, 1983.
[5] S. Chakrabarty, Phys. Rev. D 54, 1306 (1996).
[6] A. Broderick, M. Prakash, and J. M. Lattimer, Astrophys. J. 537, 351 (2000).
[7] J. Boguta and A. R. Bodmer, Nucl. Phys. A292, 413 (1977); B. D. Serot and J.D. Walecka, Adv. Nucl. Phys. 16, 1 (1986).
[8] A. Rabhi, C Providência, and J. da Providência, J. Phys. G: Nucl. Part. Phys. 35,125201 (2008).
[9] F.X. Wei, G.J. Mao, C.M. Ko, L.S. Kisslinger, H. Stocker and W. Greiner, J. Phys. G **32**, 47 (2006).
[10] H. Pais, Master thesis, University of Coimbra, 2008.
[11] R. Gonzalez Felipe, A. Perez Martinez, H. Perez Rojas and M. Orsaria, Phys. Rev. C **77**, 015807 (2008).
[12] D. P. Menezes, M. Benghi Pinto, S. S. Avancini, A. Pérez Martínez, and C. Providência, Phys. Rev. C 79, 035807 (2009).
[13] N. K. Glendenning, *Compact stars*, Springer-Verlag New York , 2000.
[14] D. Bandyopadhyay, S. Chakrabarty, and S. Pal, Phys. Rev. Lett. 79, 2176 (1997).
[15] C. Y. Cardall, M. Prakash, and J. M. Lattimer, Astrophys. J. 554, 322 (2001); A. Broderick, M. Prakash and J.M. Lattimer, Phys. Lett. B 531, 167 (2002).
[16] N. K. Glendenning and S. A. Moszkowski, Phys. Rev Lett. 67, 2414 (1991).
[17] D. N. Voskresensky, M. Yasuhira, and T. Tatsumi, Phys. Lett. B 541, 93 (2002); D. N. Voskresensky, M. Yasuhira, and T. Tatsumi, Nucl. Phys. A723, 291 (2003).
[18] T. Maruyama, S. Chiba, H-J Schulze, and T. Tatsumi, Phys. Rev. D 76, 123015 (2007).

[19] M. Bocquet, S. Bonazzola, E. Gourgoulhon, and J. Novak, Astron. Astrophys. 301, 757 (1995).
[20] Guang-Jun Mao, Akira Iwamoto, and Zhu-Xia Li, Chin. J. Astron. Astrophys. Vol. 3, No. 4, 359-374 (2003).
[21] D. P. Menezes and C. Providência, Phys. Rev. C 68, 035804 (2003); I. Bombaci, I. Parenti, I. Vidaña, Astrophys. Jour. 614, 314 (2004).
[22] D. Ebert, K.G. Klimenko, Nucl. Phys. **A 728**, 203 (2003).
[23] Paulo C. C. Freire, Alex Wolszczan, Maureen van den Berg, and Jason W. T. Hessels, Astrophys. J. 679, 1433 (2008).
[24] Paulo C. C. Freire, Scott M. Ransom, Steve Bgin, Ingrid H. Stairs, Jason W. T. Hessels, Lucille Frey, Fernando Camilo, Astrophys. J. 675, 670 (2008).
[25] D. Bailin and A. Love, Phys. Rep. 107, 325 (1984); K. Rajagopal and F. Wilczek, arXiv:hep-ph/0011333v2; M. Alford, Ann. Rev . Nucl. Part. Sci. 51, 131 (2001); Riv . Nuovo Cim. 25N3, 1 (2002); T. Schaefer, arXiv:hep-ph/0304281v2; D.H. Rischke, Prog. Part. Nucl. Phys. 52, 197 (2004); Hai-cang Ren, arXiv:hep-ph/0404074v3.
[26] M. Alford and S. Reddy, Phys. Rev. D 67, 074024 (2003); P. K. Panda, D. P. Menezes, and C. Providência, Phys. Rev. C 69, 025207 (2004); P. K. Panda, D. P. Menezes, and C. Providência, Phys. Rev. C 69, 058801 (2004).
[27] K. Iida and G. Baym, Phys. Rev. D 66, 014015 (2002); E. J. Ferrer, V. de la Incera and C. Manuel, Phys. Rev. Lett. 95, 152002 (2005); E. J. Ferrer, V. de la Incera and C. Manuel, Nucl.Phys. B 747, 88 (2006); E. J. Ferrer and V. de la Incera, Phys. Rev. Lett. 97, 122301 (2006); E. J. Ferrer and V. de la Incera, Phys. Rev. D 76, 045011 (2007); E. J. Ferrer and V. de la Incera, Phys. Rev. D 76, 114012 (2007) ; J. L. Noronha and I. A. Shovkovy, Phys. Rev. D 76, 105030 (2007); K. Fukushima and H. J. Warringa, Phys. Rev .Lett. 100, 032007 (2008); D. M. Sedrakian, K. M. Shahabasyan, D. Blaschke and M. K. Shahabasyan, Astrophysics, Vol. 51, No. 4, (2008).
[28] http://www.physics.mcgill.ca/˜pulsar/magnetar/main.html
[29] I. Bombaci, I. Parenti and I. Vidaña, Astrophys. J. **614**, 314 (2004); Ignazio Bombaci, Prafulla K. Panda, Constança Providência, and Isaac Vidaña, Phys. Rev. D 77, 083002 (2008).
[30] J. E. Horvath, O. G. Benvenuto and H. Vucetich, Phys. Rev. D **45**, 3865 (1992); J. E. Horvath, Phys. Rev. D **49**, 5590 (1994); M. L. Olesen and J. Madsen, Phys. Rev. D **49**, 2698 (1994).